NeuroImage 326 (2026) 121708

Contents lists available at ScienceDirect

NeuroImage

journal homepage: www.elsevier.com/locate/ynimg

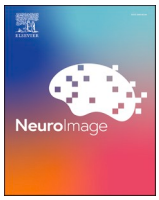

The representation of serial order in working memory: A matter of space or time?

Lucie Attout [a,*], Robin Remouchamps [b], Damien Lesenfants [b], Wim Fias [c], Steve Majerus [b]

[a] Faculty of Psychology and Educational Science, University of Geneva, Geneva, Switzerland
[b] Psychology and Neuroscience of Cognition Research Unit, University of Liège, Liège, Belgium
[c] Department of Experimental Psychology, Ghent University, Gent, Belgium

ARTICLE INFO

Keywords:
Space
Time
fMRI
Serial order
Working memory

ABSTRACT

The representation of serial order information is a fundamental aspect of verbal working memory (WM). However, the way our brain represents serial order information remains an open question. The spatial hypothesis considers that auditory-verbal serial order information is recoded using spatial codes, according to a left-to-right dimension for left-to-right readers. The temporal hypothesis considers the intervention of temporal codes for representing serial order information. This fMRI study contrasted the spatial and temporal hypotheses of WM serial order coding by administering an implicit spatial processing task involving the end-of-movement detection of a dot that stabilized on leftward, central or rightward endpoints, an implicit temporal processing task involving the detection of a target sound that occurred at early, middle and late timepoints of an auditory sequence, and a verbal WM task involving the encoding and retention of the serial order of 6-letter lists. We observed shared multivariate neural activity patterns for the encoding of WM serial position information and corresponding timepoints in the temporal processing task, and this in several frontal and parietal areas. Moreover, neural activity patterns in the left anterior IPS also distinguished the different spatial endpoints in the spatial processing task and predicted robustly corresponding serial position information in the WM task. These results provide support for implicit temporal and to a lesser extent, implicit spatial encoding of serial order information in verbal WM.

1. Introduction

Verbal serial order working memory (WM) is a fundamental cognitive ability allowing for online processing and temporary maintenance of sequential verbal information such as involved in mental calculation, problem solving or any other controlled sequential processing task. A large body of studies has highlighted the specificity of the maintenance of serial order information in WM versus item information (i.e., the linguistic or visual features of the items to be maintained, independently of their serial position in a string of information) (see Majerus, 2019 for a recent review). Moreover, the processes involved in the representation of serial order information could be potentially and partly domain-specific (see for a recent review Tian et al., 2022), although a number of neuroimaging and neurostimulation studies have documented shared neural substrates for the serial order information in verbal and visuo-spatial domains (e.g., Guidali et al., 2019; Majerus et al., 2006; 2010; Papagno et al., 2017). In this study we focused on WM for serial order information in the verbal domain in which serial order memory is most frequently studied. Most theoretical models of serial order memory also focus more specifically on serial order in the verbal domain (Hartley et al., 2016; Brown et al., 2000; Henson, 1998). At the neuroimaging level, both univariate and multivariate approaches have demonstrated the role of fronto-parietal cortices, and more specifically the intraparietal sulci (IPS), in the encoding and maintenance of serial order information (Attout et al., 2022; Cristoforetti et al., 2022; Majerus et al., 2010, 2006; Marshuetz et al., 2000).

However, the precise nature of representations that are encoded in the IPS during serial order WM tasks remain poorly understood. At the theoretical level, most computational models of WM consider that serial order is encoded by positional codes, memory items being bound to positional/contextual markers. However, the nature of these contextual markers highly differs between models (Majerus & Attout, 2018). A first

* Corresponding author.
E-mail addresses: lucie.attout@unige.ch (L. Attout), robin.remouchamps@uliege.be (R. Remouchamps), damien.lesenfants@uliege.be (D. Lesenfants), wim.fias@ugent.be (W. Fias), smajerus@uliege.be (S. Majerus).

https://doi.org/10.1016/j.neuroimage.2026.121708
Received 20 November 2025; Received in revised form 6 January 2026; Accepted 7 January 2026
Available online 8 January 2026

type of markers is defined by a spatial coding mechanism (van Dijck & Fias, 2011), with earlier memory items considered to be associated with the leftward positions of a spatial mental line and end-of-list items being associated with rightward positions (for left-to-right readers). This hypothesis is supported by a number of empirical findings. Recall/-recognition of items from the start of a word list is faster for left-hand responses and the same is true for right-hand responses to items from the end of a word list (Guida & Campitelli, 2019; van Dijck & Fias, 2011). This have led to the spatial whiteboard hypothesis suggesting that the representation of serial order information in WM would be supported by mapping the serial position of each item of a memory sequence onto an internal spatial frame characterized by a preferential horizontal mapping from left to right in participants of Western culture (Abrahamse, Van Dijck, Majerus, & Fias, 2014; Guida et al. 2020). Other evidence based on neuroimaging, electrophysiological and eye movement data is also in favor of spatial hypothesis of serial order coding (Attout et al., 2022; Rasoulzadeh et al., 2021; Sahan et al., 2022). A recent study showed that the recall of serial order information in verbal WM shares the same neurophysiological signatures as those characterizing specific spatial attention processes (Rasoulzadeh et al., 2021). The authors observed specific neural EEG signals for early vs. late items in parietal cortices linked to spatial processes as well as in premotor and frontal eye field areas linked to shifts of attention. Interestingly, early and late positions were associated with an electrophysiological marker contralateral to the position of the item in the mental space. This is also supported by more direct observation of this horizontal shift via the use of oculometry, showing leftward oculomotor movements for the retrieval of start-of-list items and rightward oculomotor movements for the retrieval of end-of-list items in WM (Sahan et al., 2022; Schroth et al., 2025). This study indicates the existence of a spatial shift toward the right or the left side of the space when information from the start or the end of a memory list is being retrieved. The left-right direction of the scanning during the encoding is confirmed by several studies showing for example an initial leftward gaze bias when participants heard an item (number) or a natural tendency to code items in a left-right direction when items were presented centrally (Sahan et al. 2022; Guida et al. 2020). Moreover, De Belder et al. (2019), by directly manipulating covert attention, observed facilitated retrieval of items from the start of a WM sequence after a spatial cue appearing on thef left side of the display and facilitated retrieval of items from the end of a WM sequence after spatial cueing of theright side. More generally, neuroimaging studies reveal that the fronto-parietal areas associated with serial order WM at least partially overlap those known to be involved in spatial attention processes (Corbetta et al., 2000; Gillebert et al., 2011; Majerus et al., 2012, 2018; Todd & Marois, 2004). However, other data indicate that spatial coding of serial order WM may be context-dependent. A literature review showed that spatial indices of serial order coding are observed only when the number of items to maintain is restricted to 4 or 5 items but not for longer WM lists (Guida et al., 2018). Moreover, this effect seems also dependent of the task presentation format, a centrally based or left-to-right item presentation during encoding leading to the established advantage for left vs. right hand/key responses, while the reverse is observed when items are presented from right to left during encoding (Guida et al., 2020). Finally, the nature of the material may also condition the use of spatial coding, spatialization effects being observed mainly for stimuli that can be processed semantically such as concrete words (Ginsburg et al., 2017). These results suggest a contextual dependency of the intervention of spatial codes in verbal WM and question their automatic use.

A second type of serial position markers are temporal codes, with successive memory items being associated with a different state of dynamic temporal signal (Brown et al., 2000; Hartley et al., 2016; Henson, 1998). This account is supported by several studies showing the influence of temporal variables on serial order WM (Fanuel et al., 2018; Henson et al., 2003; Plancher et al., 2018; Saito, 2001). A series of studies have observed that the presentation of a regular temporal signal (beat) during the encoding of a WM list improves subsequent WM recall performance while an irregular rhythm affects serial order recall, suggesting that a regular pattern of time facilitates the binding between a serial order position and a specific temporal state (Fanuel et al., 2018; Henson et al., 2003; Plancher et al., 2018). In the same vein, individual difference in reproducing temporal rhythms predict individual differences in verbal WM performance (Gilbert et al., 2017; Saito, 2001). Also, time-based computational models of serial order are able to accurately reproduce different hallmark serial order WM effects (e.g., recency and primacy effects, transposition gradients for serial order errors with an increase of serial position exchanges for adjacent positions) by associating each item with the time-evolving state of a specific (absolute or relative) temporal context signal (Brown & Chater, 2007; Brown et al., 2000; Hartley et al., 2016). The Start-end Model (Henson, 1998), as a simplified temporal model, considers that each item of a memory list is associated to start and end markers, the relative strength of association with each marker depending on the serial position of the item in the list. At the neuroimaging level, a series of studies on duration estimation, temporal accumulation and temporal preparation observed the involvement of a right-lateralized fronto-parietal network, including the IPS, the premotor cortex and the SMA areas that are also typically involved in serial order WM tasks (Coull et al., 2015; Dormal et al., 2012; Pouthas et al., 2005; Sokolowski et al., 2017). At the same time, we do not know whether temporal coding in serial order WM is a direct and specific process or whether it is mediated via the mapping of time to space, as assumed by the common magnitude hypothesis for the representation of time and space (Casasanto & Boroditsky, 2008; Walsh, 2003). Fischer-Baum and Benjamin (2014) observed better WM performance when spatial and temporal aspects of WM list encoding and recall converged (i.e., left-to-right presentation and forward as opposed to backward recall). Several neuroimaging studies (Cona et al., 2021; Fias et al., 2003; Riemer et al., 2024; Skagerlund et al., 2016) also showed overlapping neural substrates for spatial and temporal judgments, including in mainly right-lateralized areas of the IPS, the insula, the premotor cortex/SMA and the inferior frontal gyrus.

In sum, there is evidence for both spatial and temporal coding of serial order information in WM but whether the two codes are used in a separate manner to represent serial order information, whether they represent a single coding dimension or whether one of the codes is used preferentially remain open questions. Moreover and importantly, most of the previous studies assessed the spatial and the temporal representation with explicit tasks, requiring, in addition to a pure spatial or temporal representation, some ordering/magnitude processes to judge the longest temporal sequence or the largest length among several representations (Coull & Nobre, 1998; Li et al., 2012; Skagerlund et al., 2016). If temporal and/or spatial codes are the fundamental codes used to encode serial order information, then they should get recruited in an automatic, non-strategic manner. It is therefore important that the tasks used to localize temporal and spatial representations also activate these representations in a direct, non-strategic manner.

This fMRI study contrasted the temporal and spatial coding hypotheses of serial order in WM, by comparing the neural activity patterns associated with early vs. middle vs. late serial positions in a WM task, relative to neural activity patterns associated with early vs. middle vs. late time points in a temporal detection processing task on the one hand, and with movements toward the left vs. central vs. right locations in a dot-stop detection spatial processing task on the other hand. The temporal task was specifically designed to catch three successive time points (start, middle, end) of a temporal sequence along the temporal hypothesis of serial order coding in WM by assuming that successive serial positions correspond to successive time points in a temporal signal, as suggested by the time-based models of serial order WM (Henson, 1998; Hartley et al., 2016; Brown et al., 2000). Participants were instructed to identify the occurrence of a higher-pitched sound embedded within a series of lower-pitched sounds, without making an explicit judgment about its temporal location, in order to mimic the

incidental processing of temporal information when encoding items and their serial position in WM. During the WM recognition phase, each probed item was assumed to reactivate its relative association strength with start and end markers of the list. If this type of temporal codes supports the representation and retrieval of serial order position information in WM, then the multivariate neural signals discriminating start vs. end positions in the temporal task should also be able to discriminate early vs. late serial positions in the WM task, at encoding and retrieval stages.

The spatial task was specifically designed to catch spatial attentional shifts toward the left side or towards the right side. In line with the spatial whiteboard hypothesis for serial order in WM, the representation of serial order information in WM would be supported by mapping the serial position of each item of a memory sequence onto an internal spatial frame characterized by a preferential horizontal mapping from left to right in participants of Western culture (Abrahamse, Van Dijck, Majerus, & Fias, 2014; Guida et al. 2020; see Sahan et al., 2022 for a more direct observation of this horizontal shift via the use of oculometry). Therefore, we instantiated the spatial hypothesis by designing a task requiring participants to follow a dot moving on a horizontal axis, and thus to perform a leftward or rightward eye movement, or keeping their eyes focused on the centre of the screen, depending on the type of dot movement. Again, participants were instructed to detect when a dot stops without making any explicit judgment about its final spatial position in order to mimic the implicit use of spatial codes for representing serial order information in WM. During the encoding phase, we expected a horizontal left-to-right mapping of the serial position information for each successive item during memory list presentation. During the recognition phase, we expected a leftward or a rightward spatial attention shift depending on whether a serial position from the beginning or from the end of the memory list was probed.

We determined the shared or distinct nature of multivariate neural codes associated with serial order, temporal and spatial positional representations via between-task prediction of multivariate neural codes associated with corresponding positional information in each task. Moreover, we focused specifically on the encoding vs. recognition phases of the WM task for the three different serial positions, since different assumptions can be made in function of the theoretical model. Since the sequential presentation of items in a verbal WM task is inherently dependent on time, encoding of serial order information may be preferentially sustained by temporal codes while the recognition phase may involve spatial codes to a larger extent, following temporal-to-spatial recoding of serial position information during the maintenance phase.

2. Materials and methods

The full stimulus sets for the materials used in the present experiments, anonymized data files and Matlab analysis scripts are available on the Open Science Framework (https://osf.io/muwjd).

2.1. Participants

Thirty French-speaking young adults (2 left-handed) with no history of neurological disorder, sensory impairment or learning difficulties were recruited for this study. They received 10 euros per hour as a compensatory fee for their participation. Data from 1 participant had to be excluded because of excessive movement in the scanner (i.e., see criteria below). The data from 29 participants (17 women) were retained for analysis (mean age = 22.41 ± 3.06 years old, age range = 18-30). Minimal number of years of education was 12. Sample size estimation was based on an indicative design analysis in order to determine the sensitivity of a given Bayesian statistical design: this design analysis estimates the probability of obtaining a specific BF value for a specific effect as a function of simulated sample sizes and an a priori estimation of the effect size (Schönbrodt & Wagenmakers, 2018). Monte Carlo simulations and the Bayesian Factor Design Analysis available on http://shinyapps.org/apps/BFDA/ indicated that on average, a sample of 29 participants allowed to obtain a minimal Bayesian value of 3 in favour of above-chance level multivariate classifications (if H1 is true) or in favour of chance-level classification (if H0 is true) (parameters; a priori effect size of Cohen's d = .50, paired t-test, default Cauchy prior distribution). In line with the Declaration of Helsinki, all participants gave their written informed consent prior to inclusion in the study. The ethics committee of the Faculty of Medicine of the University of Liège had approved the study (2018/332).

2.2. Task description

Fig. 1 illustrates the three tasks.

The serial order WM task included three phases: (1) the encoding phase, consisting of the sequential presentation of 6 letters at the centre of the screen. Each letter was presented for 750 ms, followed by a 250 ms ISI; (2) the maintenance phase, consisting of the presentation of a fixation cross for 3000 ms; (3) the recognition phase consisting of the presentation of two probe letters organized vertically for 4000 ms maximum. The participants had to judge whether the serial order of these two letters was the same as in the memory list or not (i.e., whether the top letter had occurred before the lower letter in the memory list) by pressing the button under the middle finger for 'yes' and by pressing the button under the index for 'no'. In order to eliminate the possibility that similarities between tasks other than the spatial or temporal codes could explain inter-task prediction, we used structurally different task presentations for the WM task and the spatial and temporal tasks. In the recognition phase, we presented the WM probes vertically, to expressly avoid a similar perceptual spatial setup of the stimuli as in the spatial task given that we aimed at examining to what extent the spatial task can predict internal, mental spatial codes assumed to be associated with WM serial position information (Guida et al., 2020). Likewise, we presented the WM probes simultaneously to avoid direct perceptual similarities between the temporal structure of stimulus presentation in the WM and temporal task. No explicit start-middle-end position judgment had to be made. The two probe letters systematically came from two adjacent positions of the memory list, distributed equally over start-of-list (positions 1 and 2), middle of the list (positions 3 and 4) and end-of-list (positions 5 and 6) positions. There were 24 positive probes per serial position category, 6 positive filler trials (intermediate positions 2-3 and 4-5) and 18 negative trials; for the negative trials, the order of the two adjacent letters was reversed relative to their order in the memory list. The main analyses targeted positive trials in order to avoid contamination of neural signals by error monitoring processes; only 25% of trials involved negative probes which further allowed to optimize the ratio between task informativeness and task duration. The letters for the memory lists were sampled from the 20 consonants that define the French language. All 20 letters were sampled pseudorandomly for each serial position by applying the following constraints: (1) no letter could appear twice in the same list, (2) phonologically similar (i.e., rhyming) letters (e.g., b, c) could not appear in the same list, (3) each letter appears equally except for the letter having common rhymes with other (e.g., b, c), appearing less often.

In the Spatial dot-stop detection task, participants had to press a button when a moving white dot (3.82°) stopped on a black screen (length: 56.14°; height: 33.40°); the movement was either towards the left, either towards the right or the dot remained in a central position of the screen. Participants pressed the button under the middle finger when they noticed that the dot was in a stable leftward, central or rightward position; no explicit left-right judgment had to be made. To avoid response predictability, the travelling time (1750 ms/2000 ms/2250 ms) and the travelling distance (29.86°/36.87°/43.60° from the centre of the screen) of the dot were varied. There were 24 trials per location (left/middle/end).

In the Temporal sound detection task, a high-pitched sound (1200

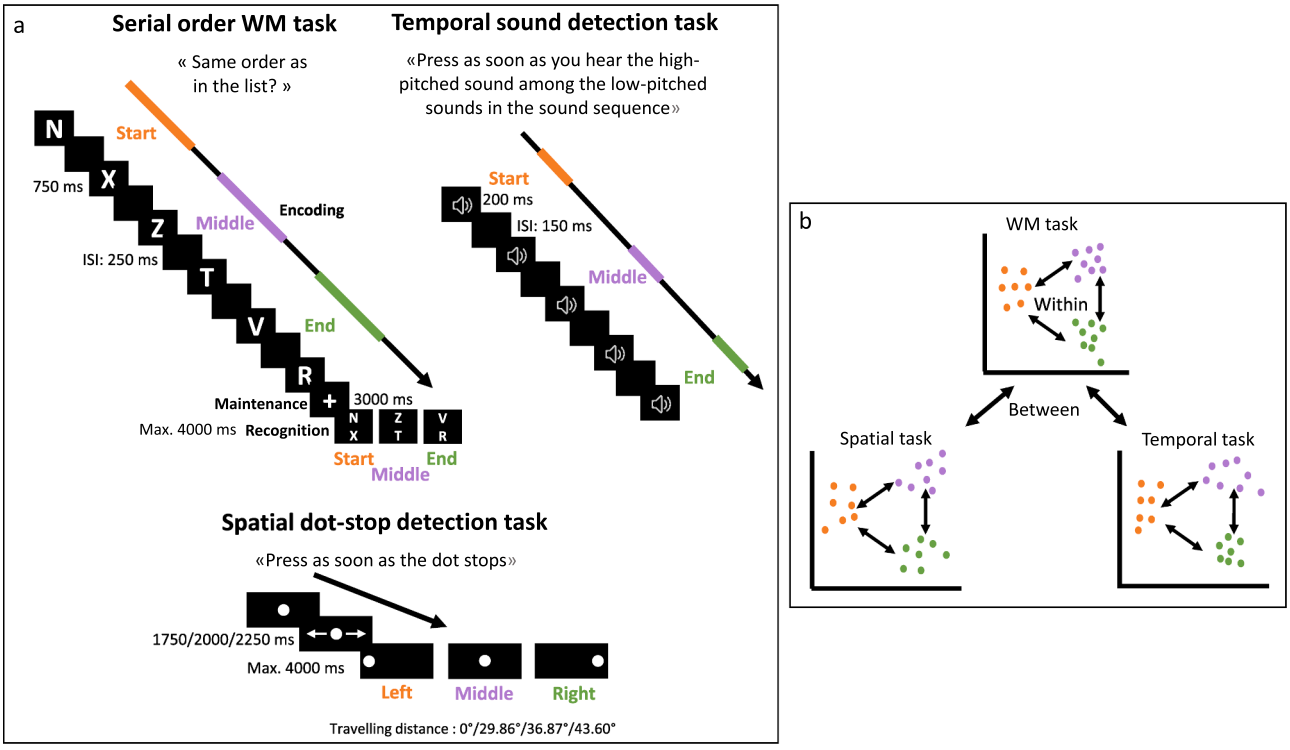

Fig. 1. Graphical summary of task design and data analysis strategy. (a) Depiction of the three different tasks administered during fMRI. Each color corresponds to one position, the start/left, the middle and the end/right. (b) Depiction of the MVPA decoding and prediction strategy. In a first step, within-task classification for the multivariate neural activity patterns associated with the three different serial/temporal/spatial position regressors was determined using a leave-one-block-out (LOBO) cross-validation procedure, for each task separately, by furthermore distinguishing between encoding and retrieval regressors in the WM task. In a second step, between-task prediction of multivariate patterns associated with the three different serial/temporal/spatial position regressors was determined using a leave-one-run-out (LORO) cross-validation procedure.

Hz, 32 bits, mono) was presented among four low-pitched sounds (600 Hz, 32 bits, mono). Each sound was played for 200 ms with an inter-trial duration of 150 ms between each sound. The participants had to press a button when they detected a high-pitched sound among a series of low-pitched sounds, the high-pitched sounds occurring either at the start of the sequence (first position), at the middle of the sequence (third position) or at the end of the sequence (fifth position). To avoid task predictability, there were also filler trials with the high-pitched sound occurring in intermediate positions (2 and 4). There were 24 trials per target position (start-1 / middle-3 / end-5) and 6 filler trials (intermediate positions, 2-4).

2.3. General procedure

Each task was presented in a single run within the same fMRI session, and the order of the three runs within each session varied randomly between participants. A black screen was presented between each trial for 7000 ± 750 ms (inter-trial interval) and before the start of each trial, an exclamation mark was presented for 750 ms to warn the participant that a new trial started. A practice session outside the scanner, prior to the start of the experiment, familiarized the participants with the specific task requirements and included the administration of at least 4 practice trials for each task until the participants demonstrated full understanding of the different tasks. The tasks were presented on a workstation running Matlab 12 and the Cogent toolbox (UCL, http://www.vislab.ucl.ac.uk/cogent.php).

2.4. fMRI method

2.4.1. MRI acquisition

Functional MRI time series were acquired on a whole-body 3T scanner (Magnetom Prisma, Siemens Medical Solutions, Erlangen, Germany) operated with a 20-channel receiver head coil. Multislice T2*-weighted functional images were acquired with the multi-band gradient-echo echo-planar imaging sequence (CMRR, University of Minnesota) using axial slice orientation and covering the whole brain (32 slices, multiband factor = 2, FoV = 192 × 192 mm^2, voxel size 3 × 3 × 3 mm^3, 25% interslice gap, matrix size 64 × 64 × 32, TR = 1174 ms, TE = 30 ms, FA = 90°). The five initial volumes were discarded to avoid T1 saturation effects. A gradient-recalled sequence was applied to acquire two complex images with different echo times (TE = 10.00 and 12.46 ms respectively) and generate field maps for distortion correction of the echo-planar images (EPI) (TR = 634 ms, FoV = 192 × 192 mm^2, 64 × 64 matrix, 40 transverse slices (3 mm thickness, 25% inter-slice gap), flip angle = 90°, bandwidth = 260 Hz/pixel). For anatomical reference, a high-resolution T1-weighted image was acquired for each subject (T1-weighted 3D magnetization-prepared rapid gradient echo (MPRAGE) sequence, TR = 1900 ms, TE = 2.19 ms, inversion time (TI) = 900 ms, FoV = 256 × 240 mm^2, matrix size = 256 × 240 × 224, voxel size = 1 × 1 × 1 mm^3). Between 592 and 704 functional volumes were acquired during the dot detection task, between 605 and 798 during the sound detection task and between 1469 and 1712 functional volumes were acquired during order WM task. Head movement was minimized by restraining the participant's head using a vacuum cushion. Stimuli were displayed on a screen positioned at the rear of the scanner, which the participant could see through a mirror mounted on the standard head coil.

2.4.2. Image preprocessing

The functional images were preprocessed using SPM12 software (Wellcome Department of Imaging Neuroscience, www.fil.ion.ucl.ac.uk/spm) implemented in MATLAB (Mathworks, Inc., Sherbom, MA).

EPI time series were corrected for motion and distortion using the Realign and Unwarp with default settings functions together with the FieldMap toolbox (implemented in SPM12) (Andersson et al., 2001; Hutton et al., 2002). A mean realigned functional image was then calculated by averaging all the realigned and unwarped functional scans and the structural T1 image was coregistered to this mean functional image (using a rigid body transformation optimised to maximise the normalised mutual information between the two images). The mapping from subject to MNI space was estimated from the structural image with the Unified segmentation approach (Ashburner & Friston, 2005). The warping parameters were then separately applied to the functional and structural images to produce normalised images of resolution $2 \times 2 \times 2$ mm^3 and $1 \times 1 \times 1$ mm^3, respectively. Finally, the warped functional images were spatially smoothed with a Gaussian kernel of 4 mm FWHM to improve signal-to-noise ratio while preserving the underlying spatial distribution (Schrouff et al., 2012); this smoothing also diminishes the impact of residual head motion can have on MVPA performance, even after head motion correction (Gardumi et al., 2016). We screened extreme head motion by excluding the entire data set of a participant if whole session movement was larger than 4 mm / 4° and/or if there was a peak movement exceeding 3 mm / 3° relative to initial head position. This resulted in the removal of the data of one participant. Note that consistent with prior work, gradual head displacements up to 4 mm were considered acceptable, slow drifts being typically well corrected by the realignment procedures and are less likely to introduce significant artifacts (see for example, Kaufmann et al. 2009; Sommerauer et al. 2020). However, participants exhibiting transient motion spikes exceeding 3 mm in any direction were excluded, as such abrupt displacements are known to introduce non-correctable artifacts and compromise data quality (Power et al., 2012). Framewise displacement (FD) was calculated to index volume-to-volume displacement in the head position. No participant obtained a mean FD higher than 0.28 (mean = 0.17, SD = 0.04) with no more than 4.06% (mean = 0.29, SD = 0.62) of volumes with a FD higher than 0.9 (standard criteria). Moreover, note that we reran the analyses reported in this manuscript with only the 23 participants showing strictly no slow or peak head movement larger than 3 mm, leading to the same pattern of results as reported here with the full sample.

2.4.3. fMRI analyses

The multivariate analyses of the 4-mm smoothed functional images were conducted using PRoNTo, a pattern recognition toolbox for neuroimaging (www.mlnl.cs.ucl.ac.uk/pronto; Schrouff et al., 2013), to determine the neural activity patterns associated with the three serial/spatial/temporal positions in the three different tasks. The following events-of-interest were defined. For the spatial dot-stop detection task, the temporal sound detection task and the recognition trials of the WM task, the target regressor ranged from the onset of the stimulus/probe display to the participant's response. Within each task, a different regressor was defined per type of serial/spatial/temporal position (start, middle, end). For the encoding phase of the WM task, the start-position regressor covered serial positions 1 and 2, the middle-position regressor covered serial positions 3 and 4 and the end-position regressor covered serial positions 5 and 6. Each regressor had a duration of 2s, which was in the range of the durations of the spatial, temporal and WM recognition regressors. To avoid a temporal overlap between encoding serial position regressors but also to work with the same number of regressors as for the recognition phase, only one of the three regressors was modelled for a given trial. For sake of comparability and consistency, we decided to model the same position regressor at the encoding stage as the one being probed at the subsequent retrieval stage. An SPM.mat file defining all individual regressors was created and then introduced into PRoNTo, on a subject-per-subject basis. First, within each task and for each participant, we trained classifiers to distinguish voxel activity patterns associated with start vs. middle vs. end positions by using a Gaussian Process Multiclass (GPC) classifier. This kind of classification use the Laplace approximation to the posterior predictive distribution (Rasmussen & Williams, 2006; Schrouff et al., 2013). We used a leave-one-block-out (LOBO) cross-validation procedure, meaning that the classifier was trained on all trials except one and tested on the left-out trial, this procedure being repeated iteratively. Second, between-task prediction was performed using a leave-one-run-out (LORO) cross-validation procedure in which the classifier was trained on the data of one of tasks and then tested on the data of another task, and vice-versa (see Fig. 1). A standard mask removing voxels outside the brain was applied to all images, and all models included timing parameters for HRF delay (5 s) and HRF overlap (5 s) ensuring that stimuli from different categories falling within the same 5 s were excluded (Schrouff et al. 2013). For each type of classification/prediction, classifier performance was tested at the group-level by comparing the group-level distribution of classification accuracies to a chance-level distribution using Bayesian one sample t-tests with Version 0.10.2.0 of the JASP software package, using default settings for the Cauchy prior distribution (JASP Team, 2017, jasp-stats.org). Individual-level within-domain and between-domain statistical classifier performance was additionally assessed using Bayesian binominal tests, which determined evidence for above chance-level individual classification accuracy at $BF_{10} > 3$. The whole-brain multivariate analyses were followed up by targeted ROI analyses covering specific brain parts of the premotor cortex, the middle and inferior frontal gyrus, the IPS, the left SMG, and the SMA.

2.4.4. ROI analyses

As indicated in the Introduction section, ROIs were selected based on their previously documented involvement in serial order WM, spatial and temporal processing tasks. Parietal ROIs covered specific subareas shown to be more specifically involved in serial order WM and cross-domain ordinal processing (Attout et al., 2022; Attout et al. 2014; Fias et al., 2007; Franklin & Jonides, 2009; Ischebeck et al., 2008; Knops & Willmes, 2013; Majerus et al., 2006), such as the anterior (hIP1 & 2) and posterior (hIP6, 7 & 8) IPS for each hemisphere. We also included two frontal ROIs that have shown a specific sensitivity to ordinal processes, situated in the bilateral middle frontal (MFG) and inferior frontal (IFG) gyri (Attout et al., 2014; Attout et al., 2022, 2015; Kalm & Norris, 2014; Majerus et al., 2010, 2006; Marshuetz et al., 2000; Martinez Perez et al., 2015). We extended the ROIs also to other cortical and subcortical regions that have been more specifically associated with WM serial order processing. These ROIs were: the bilateral premotor cortex (preSMA) (Henson et al., 2000; Kalm & Norris, 2014), the left supramarginal gyrus (SMG) (Kalm & Norris, 2014; Zhou et al., 2021) and the bilateral supplementary motor cortex (SMA) (Attout et al., 2019; Martinez Perez et al., 2015; Zhou et al., 2021). Except for the frontal and the SMG ROIs, defined via the AAL atlas, all other ROIs were defined via the SPM Anatomy toolbox and the Jülich-Brain Atlas (http://www.fz-juelich.de/).

3. Results

3.1. Behavioral analyses

For all tasks, response accuracy and response times (RT) are presented in Table 1. For the WM task, RTs are reported for correct trials, by keeping only RTs within a range of ±2.5 SD of an individual's performance (non-included RTs: 2.07%). For the two detection tasks, accuracy was expected to be at ceiling, and the RTs are presented for the sake of information. Given that participants could respond as soon as they had made a decision about spatial direction or occurrence of a high-pitched tone, including before a dot movement actually stopped in the spatial task, the RTs were naturally associated with a high variability. The effect of WM position was examined via Bayesian repeated measures ANOVA (Positions: start-middle-end) on response accuracy and response times. For accuracy, we observed no reliable effect of target serial position

Table 1
Descriptive behavioural results for the different fMRI tasks.

			Mean	SD	Minimum	Maximum
Serial order WM	Accuracy	Start	0.90	0.09	0.67	1.00
		Middle	0.87	0.08	0.74	1.00
		End	0.90	0.09	0.68	1.00
	Response Times (ms)	Start	1587.98	474.68	642.46	2539.42
		Middle	2102.38	704.19	699.05	3564.36
		End	1801.70	513.09	668.96	2702.80
Spatial dot-stop detection	Accuracy	Left	1.00	0.00	1.00	1.00
		Middle	1.00	0.00	1.00	1.00
		Right	1.00	0.00	1.00	1.00
	Response Times (ms)	Left	68.93	92.18	1.21	463.42
		Middle	524.53	193.26	191.50	1188.32
		Right	64.87	88.36	0.54	425.46
Temporal sound detection	Accuracy	Start	0.98	0.03	0.88	1.00
		Middle	1.00	0.00	1.00	1.00
		End	0.99	0.01	0.96	1.00
	Response Times (ms)	Start	688.91	178.05	455.78	1141.96
		Middle	351.21	53.95	279.65	498.58
		End	276.49	101.52	104.67	552.48

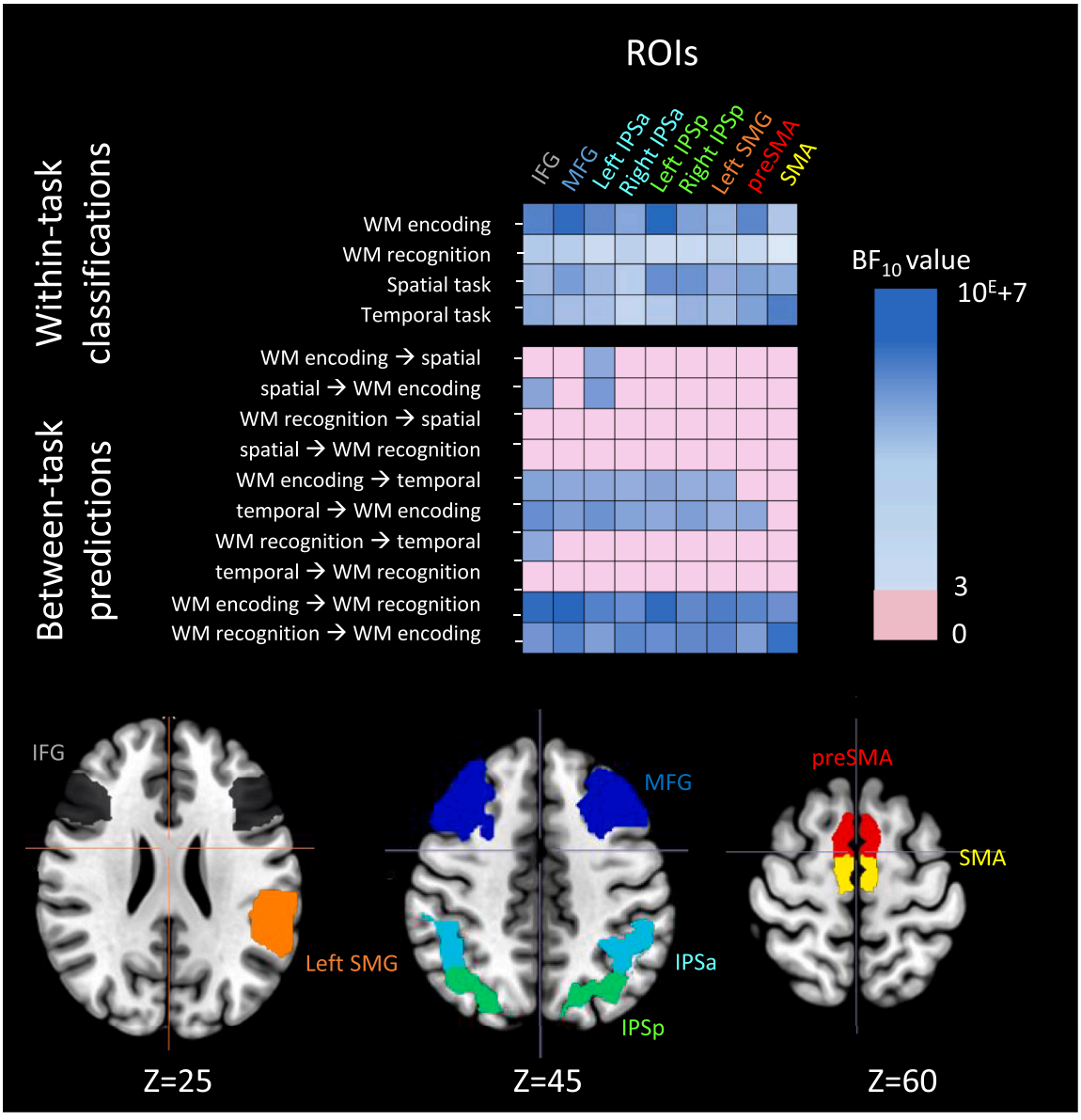

Fig. 2. Bayes Factor values for GPC multiclass decoding of type of position, for within-task (top panel) classifications and between-task (middle panel) predictions. The bottom panel depicts the selected ROI masks for the MVPA analyses.

($BF_{10} = 0.45$, $n_p^2 = 0.06$) due to the expected high levels of performance in the task overall (mean = 0.88, SD = 0.06). Regarding response times, we observed evidence in favor of a main position effect (BF_{10} = 1.82E+5, n_p^2 = 0.45), start and end position trials leading to faster response times than middle position trials, reflecting the well-known recency and primacy effects.

3.2. Neuroimaging - within-task classifications of ordinal distance

We first conducted within-task multiclass decoding analyses for the three positions (start/left, middle and end/right positions) for the different ROIs (see Fig. 2 and Table 2 for means and effect sizes), we observed above-chance level classifications of position in all ROIs and for each task (encoding phase of WM, recognition phase of WM, spatial and temporal tasks), including the premotor cortex, the IFG, the MFG, the IPSa and IPSp, the left SMG and the SMA.

3.3. Neuroimaging - between-task predictions

Next, we examined the critical between-task predictions of position for the different ROIs (see Fig. 2 and Table 3). For the prediction of position between the WM encoding phase and the temporal task, we observed robust evidence in favor of bidirectional, above-chance level prediction of position in the left and the right IPSa and IPSp, the IFG, the MFG and the left SMG. A between-task bidirectional prediction between the WM encoding phase and the spatial task in the left IPSa was also observed. No reliable bidirectional predictions were observed in the other ROIs. However, unidirectional predictions of position were observed, from the spatial task to the encoding phase of the WM task in another area such as in the IFG, from the temporal task to the encoding phase of the WM task in the preSMA and from the recognition phase of the WM task to the temporal task in the IFG.

Table 2
Classification rates of GPC multiclass classifiers of type of position in each classification (within-task) at the ROIs level.

		Mean	SD	BF_{10}	Cohen's d
IFG	WM encoding	0.51	0.08	1.74E+10	2.28
	WM recognition	0.41	0.08	2195.07	0.95
	Spatial task	0.41	0.06	266247.69	1.31
	Temporal task	0.43	0.07	4.88E+6	1.54
MFG	WM encoding	0.54	0.08	6.80E+11	2.67
	WM recognition	0.41	0.09	990.41	0.89
	Spatial task	0.46	0.07	8.91E+7	1.78
	Temporal task	0.44	0.09	48918.09	1.18
Left IPS anterior	WM encoding	0.48	0.07	5.13E+9	2.16
	WM recognition	0.39	0.09	26.77	0.61
	Spatial task	0.41	0.06	213649.32	1.29
	Temporal task	0.42	0.08	18945.96	1.11
Right IPS anterior	WM encoding	0.47	0.09	1.30E+7	1.62
	WM recognition	0.40	0.08	375.19	0.82
	Spatial task	0.39	0.07	801.92	0.87
	Temporal task	0.40	0.11	74.33	0.69
Left IPS posterior	WM encoding	0.54	0.08	1.12E+12	2.72
	WM recognition	0.39	0.10	23.86	0.60
	Spatial task	0.52	0.09	2.24E+9	2.08
	Temporal task	0.41	0.08	2662.93	0.96
Right IPS posterior	WM encoding	0.50	0.10	4.39E+7	1.72
	WM recognition	0.39	0.09	33.63	0.63
	Spatial task	0.51	0.09	9.63E+8	2.00
	Temporal task	0.43	0.07	9.55E+5	1.41
Left SMG	WM encoding	0.46	0.09	4.83E+5	1.36
	WM recognition	0.39	0.08	216.58	0.77
	Spatial task	0.42	0.06	2.02E+6	1.47
	Temporal task	0.43	0.08	1.26E+5	1.25
preSMA	WM encoding	0.51	0.08	8.04E+9	2.20
	WM recognition	0.38	0.08	41.17	0.64
	Spatial task	0.43	0.06	5.45E+7	1.74
	Temporal task	0.47	0.08	4.90E+7	1.73
SMA	WM encoding	0.43	0.10	4537.43	1.00
	WM recognition	0.36	0.08	2.28	0.38
	Spatial task	0.40	0.05	3.06E+6	1.50
	Temporal task	0.47	0.06	3.30E+10	2.34

4. Discussion

This study examined the spatial versus temporal nature of codes involved in the representation of serial order information in WM. For the prediction of position between the WM encoding phase and the temporal task, we observed robust evidence in favor of bidirectional, above-chance level prediction of position in the left and the right IPSa and IPSp, the IFG, the MFG and the left SMG. A between-task bidirectional prediction between the WM encoding phase and the spatial task was also observed in the left IPSa. No reliable bidirectional predictions were observed for the other ROIs. Additional unidirectional predictions of position were observed, from the spatial task to the encoding phase of the WM task in the IFG, from the temporal task to the encoding phase of the WM task in the preSMA and from the recognition phase of the WM task to the temporal task in the IFG.

The present results highlight the similarity of neural codes associated with the encoding of serial order information in WM and implicit temporal representational processes. Our data provide novel support to previous work suggesting a role for temporal coding in serial order WM (De Belder et al., 2017; Fanuel et al., 2018; Gilbert et al., 2017; Hartley et al., 2016; Henson et al., 2003; Plancher et al., 2018; Saito, 2001; Skagerlund et al., 2016;). The fronto-parietal regions involved in our between-domain predictions, have been consistently involved in serial order WM coding (Majerus et al., 2006; 2010; Attout et al., 2022), and this most specifically for the left IPSa and IPSp (Attout et al., 2022, 2014; Cristoforetti et al., 2022). At the same time, these specific portions of the IPS have also been shown to be involved in duration estimation and time perception tasks (Dormal et al., 2012; Skagerlund et al., 2016; Üstün et al., 2017). With regard to the premotor cortex and the MFG, these areas have been shown to be involved in time perception (Cona et al., 2021; Wiener et al., 2010). Some studies have also associated these regions with a more general role in order processing (Fulbright et al., 2003; Soltész et al., 2007) or in a space-time gradient (Cona et al., 2021). The present study provides novel and more direct evidence for common representational processes in these fronto-parietal regions during time and serial order WM processing, by showing bidirectional predictions of multivariate neural activity patterns in these areas between both task domains. We should note here that the similarities in neural activity patterns supporting serial position encoding and implicit temporal processing cannot be explained by time-dependent drifts in BOLD signal that would be common in both tasks. For the serial order WM task, each serial position was modelled separately by moving forward the time window of the regressor as a function of the advancement of the presentation of the successive items while for the temporal processing task, the event in which critical stimuli occurred at different temporal positions was always modelled with exactly the same (non-moving) time window. Furthermore, the maximal distance between modelled positions in the WM encoding phase was 4000 ms while in the temporal task, the maximal distance between the moments at which critical stimuli could occur was 1200 ms. These results thus further suggest a commonality of relative rather than absolute temporal coding in both tasks (Harvey et al., 2020). We should nevertheless note that in additional analyses, the final position appeared to be more informative for classifications than the other positions, aligning with the recency effect frequently observed in WM studies. Moreover, at the behavioral level, RTs appeared to be shorter as the sound to be detected occurred further

Table 3
Prediction rates for between classifications for each task at the ROIs level (details of the Fig. 2).

Predictions	IFG				MFG				preSMA				SMA				Left SMG			
	Mean	SD	BF_{10}	Cohen's d	Mean	SD	BF_{10}	Cohen's d	Mean	SD	BF_{10}	Cohen's d	Mean	SD	BF_{10}	Cohen's d	Mean	SD	BF_{10}	Cohen's d
WM enc → spatial	0.34	0.06	0.77	0.25	0.33	0.05	0.21	0.01	0.31	0.05	0.07	-0.38	0.30	0.04	0.04	-0.90	0.34	0.07	0.34	0.11
spatial → WM enc	0.36	0.04	24.49	0.60	0.34	0.04	0.96	0.27	0.32	0.06	0.12	-0.14	0.32	0.07	0.11	-0.19	0.35	0.06	1.04	0.29
WM recn → spatial	0.34	0.05	0.41	0.15	0.33	0.06	0.15	-0.08	0.32	0.05	0.10	-0.22	0.33	0.05	0.25	0.05	0.34	0.05	0.30	0.09
spatial → WM recn	0.33	0.05	0.17	-0.04	0.33	0.06	0.15	-0.07	0.33	0.06	0.18	-0.03	0.34	0.08	0.38	0.13	0.34	0.06	0.33	0.11
WM enc → temp	0.37	0.07	48.35	0.66	0.37	0.07	9.57	0.52	0.35	0.05	1.12	0.30	0.32	0.05	0.13	-0.12	0.35	0.06	4.29	0.44
temp → WM enc	0.39	0.06	2932.71	0.97	0.38	0.07	67.42	0.68	0.37	0.07	10.25	0.52	0.33	0.07	0.24	0.05	0.36	0.07	4.17	0.44
WM recn → temp	0.35	0.05	8.13	0.50	0.33	0.07	0.21	0.02	0.33	0.05	0.18	-0.02	0.32	0.04	0.11	-0.18	0.33	0.06	0.26	0.06
temp → WM recn	0.34	0.07	0.29	0.09	0.32	0.06	0.10	-0.22	0.32	0.06	0.12	-0.16	0.33	0.07	0.18	-0.03	0.32	0.07	0.13	-0.13
WM enc → WM recn	0.42	0.06	$2.12^{E}+6$	1.47	0.42	0.06	$3.66^{E}+6$	1.52	0.40	0.07	11500.49	1.07	0.38	0.05	1422.61	0.92	0.41	0.06	110303.83	1.24
WM recn → WM enc	0.39	0.07	518.48	0.84	0.41	0.07	37193.44	1.16	0.39	0.08	109.49	0.72	0.39	0.05	682111.60	1.38	0.40	0.06	18768.31	1.11

Predictions	Left IPSA				Right IPSA				Left IPSP				Right IPSP			
	Mean	SD	BF_{10}	Cohen's d	Mean	SD	BF_{10}	Cohen's d	Mean	SD	BF_{10}	Cohen's d	Mean	SD	BF_{10}	Cohen's d
WM enc → spatial	0.36	0.05	10.58	0.53	0.33	0.06	0.15	-0.08	0.34	0.04	0.62	0.22	0.34	0.06	0.44	0.16
spatial → WM enc	0.37	0.05	165.24	0.75	0.32	0.04	0.10	-0.24	0.33	0.04	0.25	0.06	0.35	0.06	1.23	0.31
WM recn → spatial	0.33	0.06	0.17	-0.03	0.31	0.05	0.06	-0.48	0.34	0.06	0.29	0.08	0.33	0.06	0.22	0.02
spatial → WM recn	0.34	0.06	0.62	0.21	0.34	0.05	0.68	0.23	0.34	0.06	0.44	0.16	0.34	0.06	0.31	0.10
WM enc → temp	0.36	0.06	9.09	0.51	0.36	0.07	4.51	0.45	0.37	0.06	23.36	0.60	0.36	0.06	5.18	0.46
temp → WM enc	0.39	0.07	694.26	0.86	0.38	0.07	27.76	0.61	0.37	0.08	8.00	0.50	0.38	0.07	58.85	0.67
WM recn → temp	0.34	0.06	0.62	0.21	0.33	0.06	0.23	0.04	0.34	0.04	0.35	0.12	0.33	0.06	0.21	0.01
temp → WM recn	0.34	0.05	0.42	0.15	0.34	0.07	0.36	0.12	0.34	0.06	0.59	0.21	0.33	0.06	0.16	-0.06
WM enc → WM recn	0.41	0.07	43097.09	1.17	0.39	0.06	3065.88	0.97	0.41	0.06	$3.01^{E}+6$	1.50	0.40	0.07	8710.93	1.05
WM recn → WM enc	0.38	0.07	100.53	0.72	0.39	0.06	14901.20	1.09	0.39	0.06	3514.80	0.98	0.40	0.06	6722.21	1.03

from the start of the sequence, mimicking the typical foreperiod effect observed in temporal cognition (see for example Coull, 2009). Future studies, maximizing the different positions/events in terms of positional/temporal/spatial distance may allow for more generalized predictions across serial positions.

At a theoretical level, our findings are in line with temporal coding computational accounts of WM. These models assume that the position of each item should be associated to a specific temporal context signal whose state evolves over time, resulting in items from different serial positions being associated with different temporal context signal values (Brown et al., 2000; Hartley et al., 2016). The OSCAR or SIMPLE models (Brown & Chater, 2007; Brown et al., 2000) suggest that this context signal during encoding is marked by a start signal and evolves over time thanks to a sets of temporal oscillators operating at different frequencies. At the recall stage, the context timing signal is replayed from the start and the items that have been associated with each state of the context signal are successively retrieved. As already noted, our results also indicate that this timing signal is relative rather than absolute, given that it was the relative discrimination of the start and end parts of a temporal sequence that predicted the start vs. end serial positions of a WM sequence, and not the exact timing of the temporal sequence. This particular situation is most in line with the recent BUMP (Bottom-Up Multi-scale Population oscillator) model of serial order WM by Hartley et al. (2016). This model considers that hierarchical temporal representations are generated "on the fly" by a bottom-up signal based on a set of oscillators tuned to run on different timescales and responding to local variation of the timing signal.

While supporting the role of temporal processes in serial order WM, the present study found relatively weak evidence for a role of left-right spatial codes in the encoding and retrieval of serial order information in WM, excepted in the left anterior IPS. The left anterior IPS is specifically the area found for processing ordinal distances across different domains such as numerical, alphabetical, and WM domains (Attout et al., 2014; 2022; Goffin et al., 2020) and for processing positions (contrasted during a recall phase) in a serial order WM task (Cristoforetti et al. 2022).

The fact that the predictions from spatial codes to serial order WM codes are restricted to only one area could underlines the multidimensional nature of the codes used to represent WM serial order information, of which the spatial dimension may be a relatively secondary one. When predicting multidimensional serial order position codes by unidimensional spatial codes, the specific multivariate signals differentiating the spatial positions may well be detectable among the different dimensions that define the serial order codes, but the reverse will be more difficult to achieve especially if the spatial dimension is of relatively low expression in the multidimensional code relative to the temporal dimension. This speculative interpretation will need to be tested in future studies.

Different reasons may explain a lesser contribution of spatial codes than temporal codes to serial order decoding in WM. First, it could be argued that spatial codes are only associated to WM representations once the entire sequence has been encoded. While the mental whiteboard theoretical account of spatial coding in WM (Abrahamse et al., 2014) does not clearly address this question, it should be noted that most of the studies providing evidence for spatial representation of serial order in verbal WM focused on retention and retrieval stages of WM rather than encoding phases (Cristoforetti et al., 2022; Sahan et al., 2022; van Dijck & Fias, 2011). But if the spatial codes are associated to WM representations only at a post-encoding stage, we should have observed stronger predictions of WM serial position information by the spatial classifier at the WM *retrieval* stage, which was not the case either.

A further reason may, however, stem from possible limits of the spatial dot-stop task used in this study. During WM encoding, if spatial processes are used, they will develop in left-to-right manner. Hence, a spatial classifier that involves movements to the right but also to the left may not fully capture the spatial coding processes occurring during the sequential encoding of WM information. This critique is not valid for the WM retrieval stage, where WM probes from early list positions should induce movements to the left and WM probes from later list positions should induce movements to the right. In the same vein, the use of a variable travel distance from the starting to the end point in the spatial task may also have influenced the results. However, while the eye-tracking study of Sahan et al. (2022) suggested absolute spatial movement sizes between positions, a recent study (Schroth et al., 2025) suggests that internal spatial movements may also be relative such as rightward movements to check position 2 relative to position 1 or leftward movements to check position 5 relative to position 6. Further studies are needed to examine in a more specific manner the spatial processes occurring during processing of serial order information in WM, contrasting relative vs. static spatial representations and implicit vs. explicit spatialization processes, at both WM encoding and retrieval stages. Further studies are needed to examine in a more specific manner the spatial processes occurring during processing of serial order information in WM, contrasting relative vs. static spatial representations and implicit vs. explicit spatialization processes, at both WM encoding and retrieval stages.

Furthermore, we observed between-task prediction of serial order WM position by the temporal and the spatial tasks for the WM encoding stage but not for the WM recognition stage, when considering only bidirectional predictions. This finding suggests that the markers used to encode the serial information are not necessarily re-activated *per se* during the recognition phase. At the same time, the neural activity patterns associated with WM encoding of serial position information predicted WM recognition of the same serial position information in a highly reliable manner. This pattern of result indicates that serial order WM representations contain additional information going beyond a position-specific temporal signal. This additional information could reflect the explicit binding of a given item to its serial position and associated temporal code. It is this bound representation, rather than the raw temporal signal activated during encoding, that would further drive WM maintenance and retrieval. This interpretation is compatible with fully recurrent computational models of serial order WM such as proposed by Botvinick and Plaut (2006). This type of model considers that, following an initial sequential encoding of items, item and serial position information are encoded jointly via a distributed pattern of activations in a hidden layer, and this distributed pattern is reinstantiated at recall rather than only the initial temporal context *per se*. This interpretation is also in line with a recent two-photon calcium imaging study focusing on macaque lateral prefrontal cortex and showing that the neural representations for individuals items were dependent upon the temporal moment at which they occurred in a WM sequence (Xie et al., 2022). These findings are also consistent with other recent studies suggesting that WM representations dynamically change over the course of a WM task, with the final representation of an item involving bound item-order information and being different from the initial representation of the item when being encoded in WM (Stroud et al., 2024; Wan et al., 2024). Those results as well as our own here therefore contradict some core assumptions of context-based models of serial order WM discussed above (Burgess & Hitch, 1999; Hartley et al., 2016), these models assuming that context and item information are the same at encoding and recall.

5. Conclusion

To conclude, this study shows that the neural activity patterns associated with temporal coding allow to predict the neural activity patterns associated with the encoding of serial position information in WM, while neural patterns associated with spatial coding show a more limited prediction of WM serial position information. The present results provide support for the temporal hypothesis and in a lesser extent for the spatial hypothesis of serial order coding in WM, at least during the WM encoding stage. Future studies need to determine the fate of these codes over subsequent WM stages, as well as the extent of contribution of

spatial codes.

Ethics approval

The study was approved by the ethics committee of the Comité d'Ethique Hospitalo-Facultaire Universitaire de Liège.

Consent to participate

Informed consent was obtained from all individual participants included in the study.

Consent for publication

Not applicable.

Funding

This work was supported by a grant from the Belgian National Fund for Scientific Research FRS-FNRS (Grant EOS 30446199 and CR, FC 88264).

Data availability

The full stimulus sets for the materials used in the present experiments, anonymized data files and Matlab analysis scripts are available on the Open Science Framework (https://osf.io/muwjd).

CRediT authorship contribution statement

Lucie Attout: Writing – review & editing, Writing – original draft, Visualization, Software, Project administration, Methodology, Investigation, Funding acquisition, Formal analysis, Data curation, Conceptualization. **Robin Remouchamps:** Data curation. **Damien Lesenfants:** Software, Formal analysis. **Wim Fias:** Writing – original draft, Methodology. **Steve Majerus:** Writing – review & editing, Writing – original draft, Validation, Supervision, Resources, Project administration, Methodology, Funding acquisition, Conceptualization.

Declaration of competing interest

The authors declare that they have no known competing financial interests or personal relationships that could have appeared to influence the work reported in this paper.

Acknowledgments

We would like to thank all participants for their time and effort invested in this study.

References

Abrahamse, E.L., van Dijck, J., Majerus, S., Fias, W., 2014. Finding the answer in space : the mental whiteboard hypothesis on serial order in working memory. Front. Hum. Neurosci. 8, 932. https://doi.org/10.3389/fnhum.2014.00932.

Andersson, J.L., Hutton, C., Ashburner, J., Turner, R., Friston, K., 2001. Modeling geometric deformations in EPI time series. NeuroImage 13 (5), 903–919. https://doi.org/10.1006/nimg.2001.0746.

Ashburner, J., Friston, K.J., 2005. Unified segmentation. NeuroImage 26 (3), 839–851. https://doi.org/10.1016/j.neuroimage.2005.02.018.

Attout, L., Fias, W., Salmon, E., Majerus, S., 2014. Common neural substrates for ordinal representation in short-term memory, numerical and alphabetical cognition. PloS One 9 (3). https://doi.org/10.1371/journal.pone.0092049.

Attout, L., Leroy, N., Majerus, S., 2022. The neural representation of ordinal information: domain-specific or domain-general? Cereb. Cortex 32 (6), 1170–1183. https://doi.org/10.1093/cercor/bhab279.

Attout, L., Ordonez Magro, L., Szmalec, A., Majerus, S., 2019. The developmental neural substrates of item and serial order components of verbal working memory. Hum. Brain Mapp. 40 (5), 1541–1553. https://doi.org/10.1002/hbm.24466.

Attout, L., Salmon, E., Majerus, S., 2015. Working memory for serial order is dysfunctional in adults with a history of developmental dyscalculia : evidence from behavioral and neuroimaging data. Dev. Neuropsychol. 40 (4), 230–247. https://doi.org/10.1080/87565641.2015.1036993.

Brown, G.D.A., Chater, N., 2007. A temporal ratio model of memory 114 (3), 539–576. https://doi.org/10.1037/0033-295X.114.3.539.

Botvinick, M.M., Plaut, D.C., 2006. Short-term memory for serial order: a recurrent neural network model. Psychol. Rev. 113 (2), 201–233. https://doi.org/10.1037/0033-295X.113.2.201.

Brown, G.D.A., Preece, T., Hulme, C., 2000. Oscillator-based memory for serial order. Psychol. Rev. 107 (1), 127–181. https://doi.org/10.1037//0033-295X.107.1.127.

Burgess, N., Hitch, G.J., 1999. Memory for serial order: a network model of the phonological loop and its timing. Psychol. Rev. 106 (3), 551–581. https://doi.org/10.1037/0033-295X.106.3.551.

Casasanto, D., Boroditsky, L., 2008. Time in the mind: using space to think about time. Cognition 106 (2), 579–593. https://doi.org/10.1016/j.cognition.2007.03.004.

Cona, G., Wiener, M., Scarpazza, C., 2021. From ATOM to GradiATOM: cortical gradients support time and space processing as revealed by a meta-analysis of neuroimaging studies. NeuroImage 224, 117407. https://doi.org/10.1016/j.neuroimage.2020.117407.

Corbetta, M., Kincade, J.M., Ollinger, J.M., McAvoy, M.P., Shulman, G.L., 2000. Voluntary orienting is dissociated from target detection in human posterior parietal cortex. Nat. Neurosci. 3 (3), 292–297. https://doi.org/10.1038/73009.

Coull, J.T., 2009. Neural substrates of mounting temporal expectation. PLoS Biol. 7 (8), e1000166. https://doi.org/10.1371/journal.pbio.1000166.

Coull, J.T., Charras, P., Donadieu, M., Droit-Volet, S., Vidal, F., 2015. SMA selectively codes the active accumulation of temporal, not spatial, magnitude. J. Cogn. Neurosci. 27 (11), 2281–2298. https://doi.org/10.1162/jocn_a_00854.

Coull, J.T., Nobre, A.C., 1998. Where and when to pay attention: the neural systems for directing attention to spatial locations and to time intervals as revealed by both PET and fMRI. J. Neurosci. 18 (18), 7426–7435. https://doi.org/10.1523/jneurosci.18-18-07426.1998.

Cristoforetti, G., Majerus, S., Sahan, M.I., van Dijck, J., Fias, W., 2022. Neural patterns in parietal cortex and hippocampus distinguish retrieval of start versus end positions in working memory. J. Cogn. Neurosci. 34 (7), 1230–1245. https://doi.org/10.1162/jocn_a_01860.

De Belder, M., Abrahamse, E., Kerckhof, M., Fias, W., van Dijck, J., 2019. Serial position markers in space: visuospatial priming of serial order working memory retrieval. PLOS ONE 14 (3), e0214762. https://doi.org/10.1371/journal.pone.0214762.

De Belder, M., van Dijck, J., Cappelletti, M., Fias, W., 2017. How serially organized working memory information interacts with timing. Psychol. Res. 81 (6), 1255–1263. https://doi.org/10.1007/s00426-016-0816-8.

Dormal, V., Dormal, G., Joassin, F., Pesenti, M., 2012. A common right fronto-parietal network for numerosity and duration processing: an fMRI study. Hum. Brain Mapp. 33 (6), 1490–1501. https://doi.org/10.1002/hbm.21300.

Fanuel, L., Portrat, S., Tillmann, B., Plancher, G., 2018. Temporal regularities allow saving time for maintenance in working memory. Ann. N. Y. Acad. Sci. 1424 (1), 202–211. https://doi.org/10.1111/nyas.13611.

Fias, W., Lammertyn, J., Caessens, B., Orban, G.A., 2007. Processing of abstract ordinal knowledge in the horizontal segment of the intraparietal sulcus. J. Neurosci. 27 (33), 8952–8956. https://doi.org/10.1523/JNEUROSCI.2076-07.2007.

Fias, W., Lammertyn, J., Reynvoet, B., Dupont, P., Orban, G.A., 2003. Parietal representation of symbolic and nonsymbolic magnitude. J. Cogn. Neurosci. 15 (1), 47–56. https://doi.org/10.1162/089892903321107819.

Fischer-Baum, S., Benjamin, A.S., 2014. Time, space, and memory for order. Psychon. Bull. Rev. 21 (5), 1263–1271. https://doi.org/10.3758/s13423-014-0604-7.

Franklin, M.S., Jonides, J., 2009. Order and magnitude share a common representation in parietal cortex. J. Cogn. Neurosci. 21 (11), 2114–2120. https://doi.org/10.1162/jocn.2008.21181.

Fulbright, R.K., Manson, S.C., Skudlarski, P., Lacadie, C.M., Gore, J.C., 2003. Quantity determination and the distance effect with letters, numbers, and shapes: a functional MR imaging study of number processing. Am. J. Neuroradiol. 24 (2), 193–200. http://www.ncbi.nlm.nih.gov/pubmed/12591633.

Gardumi, A., Ivanov, D., Hausfeld, L., Valente, G., Formisano, E., Uludağ, K., 2016. The effect of spatial resolution on decoding accuracy in fMRI multivariate pattern analysis. NeuroImage 132, 32–42. https://doi.org/10.1016/j.neuroimage.2016.02.033.

Gilbert, R.A., Hitch, G.J., Hartley, T., 2017. Temporal precision and the capacity of auditory–verbal short-term memory. Q. J. Exp. Psychol. 70 (12), 2403–2418. https://doi.org/10.1080/17470218.2016.1239749.

Gillebert, C.R., Mantini, D., Thijs, V., Sunaert, S., Dupont, P., Vandenberghe, R., 2011. Lesion evidence for the critical role of the intraparietal sulcus in spatial attention. Brain 134 (6), 1694–1709. https://doi.org/10.1093/brain/awr085.

Ginsburg, V., Archambeau, K., van Dijck, J., Chetail, F., Gevers, W., 2017. Coding of serial order in verbal, visual and spatial working memory. J. Exp. Psychol.: Gen. 146 (5), 632–650. https://doi.org/10.1037/xge0000278.

Goffin, C., Vogel, S.E., Slipenkyj, M., Ansari, D., 2020. A comes before B, like 1 comes before 2. Is the parietal cortex sensitive to ordinal relationships in both numbers and letters? An fMRI-adaptation study. Hum. Brain Mapp. 41 (6), 1591–1610. https://doi.org/10.1002/hbm.24897.

Guida, A., Abrahamse, E.L., van Dijck, J., 2020. About the interplay between internal and external spatial codes in the mind: implications for serial order. Ann. N. Y. Acad. Sci. 1477 (1), 1–14. https://doi.org/10.1111/nyas.14341.

Guida, A., Campitelli, G., 2019. Explaining the SPoARC and SNARC effects with knowledge structures: an expertise account. Psychon. Bull. Rev. 26 (2), 434–451. https://doi.org/10.3758/s13423-019-01582-0.

Guida, A., Carnet, S., Normandon, M., Lavielle-Guida, M., 2018. Can spatialisation be extended to episodic memory and open sets? Memory 26 (7), 922–935. https://doi.org/10.1080/09658211.2018.1428350.

Guidali, G., Pisoni, A., Bolognini, N., Papagno, C., 2019. Keeping order in the brain: the supramarginal gyrus and serial order in short-term memory. Cortex 119, 89–99. https://doi.org/10.1016/j.cortex.2019.04.009.

Hartley, T., Hurlstone, M.J., Hitch, G.J., 2016. Effects of rhythm on memory for spoken sequences: a model and tests of its stimulus-driven mechanism. Cogn. Psychol. 87, 135–178. https://doi.org/10.1016/j.cogpsych.2016.05.001.

Harvey, B.M., Dumoulin, S.O., Fracasso, A., Paul, J.M., 2020. A network of topographic maps in human association cortex hierarchically transforms visual timing-selective responses. Curr. Biol. 30 (8), 1424–1434.e6. https://doi.org/10.1016/j.cub.2020.01.090.

Henson, R.N.A., 1998. Short-term memory for serial order: the start-end model. Cogn. Psychol. 36 (2), 73–137. https://doi.org/10.1006/cogp.1998.0685.

Henson, R.N.A., Burgess, N., Frith, C.D., 2000. Recoding, storage, rehearsal and grouping in verbal short-term memory: an fMRI study. Neuropsychologia 38 (4), 426–440. https://doi.org/10.1016/S0028-3932(99)00098-6.

Henson, R.N.A., Hartley, T., Burgess, N., Hitch, G., Flude, B., 2003. Selective interference with verbal short-term memory for serial order information: a new paradigm and tests of a timing-signal hypothesis. Q. J. Exp. Psychol. 56 (8), 1307–1334. https://doi.org/10.1080/02724980244000747.

Hutton, C., Bork, A., Josephs, O., Deichmann, R., Ashburner, J., Turner, R., 2002. Image distortion correction in fMRI: a quantitative evaluation. NeuroImage 16 (1), 217–240. https://doi.org/10.1006/nimg.2001.1054.

Ischebeck, A., Heim, S., Siedentopf, C., Zamarian, L., Schocke, M., Kremser, C., Egger, K., Strenge, H., Scheperjans, F., Delazer, M., 2008. Are numbers special? Comparing the generation of verbal materials from ordered categories (months) to numbers and other categories (animals) in an fMRI study. Hum. Brain Mapp. 29 (8), 894–909. https://doi.org/10.1002/hbm.20433.

Kalm, K., Norris, D., 2014. The representation of order information in auditory-verbal short-term memory. J. Neurosci. 34 (20), 6879–6886. https://doi.org/10.1523/JNEUROSCI.4104-13.2014.

Kaufmann, L., Vogel, S.E., Starke, M., Kremser, C., Schocke, M., Wood, G., 2009. Developmental dyscalculia: compensatory mechanisms in left intraparietal regions in response to nonsymbolic magnitudes. Behav. Brain Funct. 5 (1), 35. https://doi.org/10.1186/1744-9081-5-35.

Knops, A., Willmes, K., 2013. Numerical ordering and symbolic arithmetic share frontal and parietal circuits in the right hemisphere. NeuroImage 84, 786–795. https://doi.org/10.1016/j.neuroimage.2013.09.037.

Li, C., Chen, K., Han, H., Chui, D., Wu, J., 2012. An fMRI study of the neural systems involved in visually cued auditory top-down spatial and temporal attention. PLoS One 7 (11), e49948. https://doi.org/10.1371/journal.pone.0049948.

Majerus, S., 2019. Verbal working memory and the phonological buffer: the question of serial order. Cortex 112, 122–133. https://doi.org/10.1016/j.cortex.2018.04.016 (May).

Majerus, S., Attout, L., 2018. Working memory for serial order and numerical cognition: what kind of association? In: Henik, A., Fias, W. (Eds.), Heterogeneity of Function in Numerical Cognition. Elsevier Academic Press, pp. 409–431. https://doi.org/10.1016/B978-0-12-811529-9.00019-4.

Majerus, S., Attout, L., D'Argembeau, A., Degueldre, C., Fias, W., Maquet, P., Martinez Perez, T., Stawarczyk, D., Salmon, E., Van der Linden, M., Phillips, C., Balteau, E., Argembeau, A.D., Degueldre, C., Fias, W., Maquet, P., Perez, T.M., Stawarczyk, D., Salmon, E., Balteau, E., 2012. Attention supports verbal short-term memory via competition between dorsal and ventral attention networks. Cereb. Cortex 22 (5), 1086–1097. https://doi.org/10.1093/cercor/bhr174.

Majerus, S., D'Argembeau, A., Martinez Perez, T., Belayachi, S., Van der Linden, M., Collette, F., Salmon, E., Seurinck, R., Fias, W., Maquet, P., 2010. The commonality of neural networks for verbal and visual short-term memory. J. Cogn. Neurosci. 22 (11), 2570–2593. https://doi.org/10.1162/jocn.2009.21378.

Majerus, S., Péters, F., Bouffier, M., Cowan, N., Phillips, C., 2018. The dorsal attention network reflects both encoding load and top-down control during working memory. J. Cogn. Neurosci. 30 (2), 144–159. https://doi.org/10.1162/jocn_a_01195.

Majerus, S., Poncelet, M., Van der Linden, M., Albouy, G., Salmon, E., Sterpenich, V., Vandewalle, G., Collette, F., Maquet, P., 2006. The left intraparietal sulcus and verbal short-term memory: focus of attention or serial order? NeuroImage 32 (2), 880–891. https://doi.org/10.1016/j.neuroimage.2006.03.048.

Marshuetz, C., Smith, E.E., Jonides, J., DeGutis, J., Chenevert, T.L., 2000. Order information in working memory: fMRI evidence for parietal and prefrontal mechanisms. J. Cogn. Neurosci. 12 (2), 130–144. https://doi.org/10.1162/089892900051137459.

Martinez Perez, T., Poncelet, M., Salmon, E., Majerus, S., 2015. Functional alterations in order short-term memory networks in adults with dyslexia. Dev. Neuropsychol. 40 (7–8), 407–429. https://doi.org/10.1080/87565641.2016.1153098.

Papagno, C., Comi, A., Riva, M., Bizzi, A., Vernice, M., Casarotti, A., Fava, E., Bello, L., 2017. Mapping the brain network of the phonological loop. Hum. Brain Mapp. 38 (6), 3011–3024. https://doi.org/10.1002/hbm.23569.

Plancher, G., Lévêque, Y., Fanuel, L., Piquandet, G., Tillmann, B., 2018. Boosting maintenance in working memory with temporal regularities. J. Exp. Psychol.: Learn. Mem. Cogn. 44 (5), 812–818. https://doi.org/10.1037/xlm0000481.

Pouthas, V., George, N., Poline, J.-B., Pfeuty, M., VandeMoorteele, P.-F., Hugueville, L., Ferrandez, A.-M., Lehéricy, S., LeBihan, D., Renault, B., 2005. Neural network involved in time perception: an fMRI study comparing long and short interval estimation. Hum. Brain Mapp. 25 (4), 433–441. https://doi.org/10.1002/hbm.20126.

Power, J.D., Barnes, K.A., Snyder, A.Z., Schlaggar, B.L., Petersen, S.E., 2012. Spurious but systematic correlations in functional connectivity MRI networks arise from subject motion. NeuroImage 59 (3), 2142–2154. https://doi.org/10.1016/j.neuroimage.2011.10.018.

Rasmussen, C.E., Williams, C.K.I., 2006. Gaussian Processes for Machine Learning. MIT Press.

Rasoulzadeh, V., Sahan, M.I., van Dijck, J., Abrahamse, E., Marzecova, A., Verguts, T., Fias, W., 2021. Spatial attention in serial order working memory: an EEG study. Cereb. Cortex 31 (5), 2482–2493. https://doi.org/10.1093/cercor/bhaa368.

Riemer, M., Wolbers, T., van Rijn, H., 2024. Memory traces of duration and location in the right intraparietal sulcus. NeuroImage 297, 120706. https://doi.org/10.1016/j.neuroimage.2024.120706.

Sahan, M.I., van Dijck, J., Fias, W., 2022. Eye-movements reveal the serial position of the attended item in verbal working memory. Psychon. Bull. Rev. 29, 530–540. https://doi.org/10.3758/s13423-021-02005-9.

Saito, S., 2001. The phonological loop and memory for rhythms: an individual differences approach. Memory 9 (4–6), 313–322. https://doi.org/10.1080/09658210143000164.

Schönbrodt, F.D., Wagenmakers, E.J., 2018. Bayes factor design analysis: planning for compelling evidence. Psychon. Bull. Rev. 25 (1), 128–142. https://doi.org/10.3758/s13423-017-1230-y.

Schroth, L.S.M., Fias, W., Sahan, M.I., 2025. Eye movements follow the dynamic shifts of attention through serial order in verbal working memory. Sci. Rep. 15, 1832. https://doi.org/10.1038/s41598-024-85015-6.

Schrouff, J., Kussé, C., Wehenkel, L., Maquet, P., Phillips, C., 2012. Decoding semi-constrained brain activity from fMRI using support vector machines and Gaussian processes. PLoS One 7 (4), e35860. https://doi.org/10.1371/journal.pone.0035860.

Schrouff, J., Rosa, M.J., Rondina, J.M., Marquand, A.F., Chu, C., Ashburner, J., Phillips, C., Richiardi, J., Mourão-Miranda, J., 2013. PRoNTo: pattern recognition for neuroimaging toolbox. Neuroinformatics 11 (3), 319–337. https://doi.org/10.1007/s12021-013-9178-1.

Skagerlund, K., Karlsson, T., Träff, U., 2016. Magnitude processing in the brain: an fMRI study of time, space, and numerosity as a shared cortical system. Front. Hum. Neurosci. 10, 500. https://doi.org/10.3389/fnhum.2016.00500.

Sokolowski, H.M., Fias, W., Bosah Ononye, C., Ansari, D., 2017. Are numbers grounded in a general magnitude processing system? A functional neuroimaging meta-analysis. Neuropsychologia 105, 50–69. https://doi.org/10.1016/j.neuropsychologia.2017.01.019.

Soltész, F., Szűcs, D., Dékány, J., Márkus, A., Csépe, V., 2007. A combined event-related potential and neuropsychological investigation of developmental dyscalculia. Neurosci. Lett. 417 (2), 181–186. https://doi.org/10.1016/j.neulet.2007.02.067.

Sommerauer, G., Graß, K.H., Grabner, R.H., Vogel, S.E., 2020. The semantic control network mediates the relationship between symbolic numerical order processing and arithmetic performance in children. Neuropsychologia 141, 107405. https://doi.org/10.1016/j.neuropsychologia.2020.107405.

Stroud, J.P., Duncan, J., Lengyel, M., 2024. The computational foundations of dynamic coding in working memory. Trends Cogn. Sci 28 (7), 614–627. https://doi.org/10.1016/j.tics.2024.02.011.

Tian, Y., Beier, M.E., Fischer-Baum, S., 2022. The domain-specificity of serial order working memory. Mem. Cogn. 50 (5), 941–961. https://doi.org/10.3758/s13421-021-01260-4.

Todd, J.J., Marois, R., 2004. Capacity limit of visual short-term memory in human posterior parietal cortex. Nature 428 (6984), 751–754. https://doi.org/10.1038/nature02466.

Üstün, S., Kale, E.H., Çiçek, M., 2017. Neural networks for time perception and working memory. Front. Hum. Neurosci. 11, 83. https://doi.org/10.3389/fnhum.2017.00083.

van Dijck, J., Fias, W., 2011. A working memory account for spatial-numerical associations. Cognition 119 (1), 114–119. https://doi.org/10.1016/j.cognition.2010.12.013.

Walsh, V., 2003. A theory of magnitude: common cortical metrics of time, space and quantity. Trends Cogn. Sci. 7 (11), 483–488. https://doi.org/10.1016/j.tics.2003.09.002.

Wan, Q., Ardalan, A., Fulvio, J.M., Postle, B.R., 2024. Representing context and priority in working memory. J. Cogn. Neurosci. 36 (7), 1374–1394. https://doi.org/10.1162/jocn_a_02166.

Wiener, M., Turkeltaub, P., Coslett, H.B., 2010. The image of time: a voxel-wise meta-analysis. NeuroImage 49 (2), 1728–1740. https://doi.org/10.1016/j.neuroimage.2009.09.064.

Xie, Y., Hu, P., Li, J., Chen, J., Song, W., Wang, X.J., Yang, T., Dehaene, S., Tang, S., Min, B., Wang, L., 2022. Geometry of sequence working memory in macaque prefrontal cortex. Science 375 (6581), 632–639. https://doi.org/10.1126/science.abm0204.

Zhou, D., Cai, Q., Luo, J., Yi, Z., Li, Y., Seger, C.A., Chen, Q., 2021. The neural mechanism of spatial-positional association in working memory: a fMRI study. Brain Cogn. 152, 105756. https://doi.org/10.1016/j.bandc.2021.105756.